Specific quantum mechanical/molecular mechanical capping-potentials for biomolecular functional groups

Arvid Conrad Ihrig, Christoph Schiffmann, and Daniel Sebastiani

---

Articles you may be interested in

Quantum mechanical/molecular mechanical/continuum style solvation model: Second order Møller-Plesset perturbation theory
J. Chem. Phys. 140, 174115 (2014); 10.1063/1.4873344

Quantum mechanical/molecular mechanical/continuum style solvation model: Time-dependent density functional theory
J. Chem. Phys. 139, 084106 (2013); 10.1063/1.4819139

A statistical nanomechanism of biomolecular patterning actuated by surface potential
J. Appl. Phys. 109, 034702 (2011); 10.1063/1.3533982

Improved pseudobonds for combined ab initio quantum mechanical/molecular mechanical methods
J. Chem. Phys. 122, 024114 (2005); 10.1063/1.1834899

Parallel iterative reaction path optimization in ab initio quantum mechanical/molecular mechanical modeling of enzyme reactions
J. Chem. Phys. 121, 697 (2004); 10.1063/1.1759318

Specific quantum mechanical/molecular mechanical capping-potentials for biomolecular functional groups

Arvid Conrad Ihrig, Christoph Schiffmann, and Daniel Sebastiani
Dahlem Center for Complex Quantum Systems, Physics Department, Freie Universität Berlin, Arnimallee 14, 14195 Berlin, Germany

We present a series of capping-potentials designed as link atoms to saturate dangling bonds at the quantum/classical interface within density functional theory-based hybrid QM/MM calculations. We aim at imitating the properties of different carbon-carbon bonds by means of monovalent analytic pseudopotentials. These effective potentials are optimized such that the perturbations of the quantum electronic density are minimized. This optimization is based on a stochastic scheme, which helps to avoid local minima trapping. For a series of common biomolecular groups, we find capping-potentials that outperform the more common hydrogen-capping in view of structural and spectroscopic properties. To demonstrate the transferability to complex systems, we also benchmark our potentials with a hydrogen-bonded dimer, yielding systematic improvements in structural and spectroscopic parameters. © *2011 American Institute of Physics*. [doi:10.1063/1.3664300]

I. INTRODUCTION

Molecular simulations are an important tool to understand how nature works. Classical simulations based on force fields (molecular mechanics–MM) are able to handle large systems and can for instance be used to understand the structure and dynamics of proteins.[1–5] Quantum mechanical (QM) simulations have a higher predictive power because no adjustable, empirical parameters are needed.[6–12] Both computational schemes also have their weak points: MM-simulations cannot cleave or form bonds, which is crucial for chemical reactions. QM-simulations on the other hand have much higher computational costs, limiting the system size. A self-evident way to deal with these drawbacks is to combine the two methods suitably. These QM/MM hybrid simulations model a region of interest (such as the active center of a protein) at the quantum level, while the surrounding area (in this example the remaining part of the protein) is modeled classically.[13–22]

One of the main problems, that arises in this approach, is the methodological change at the interface between the two regions,[23–26] when unsaturated bonds are created at the QM/MM boundary (see Figure 1). This bond cleavage causes a significant perturbation of the electronic structure which usually spreads across several covalent bonds. There are several established techniques to model these interfaces, for example hydrogen-capping,[27] fluorine-capping (based on a pseudobond approach[28]), effective capping potentials,[29,30] generalized hybrid orbitals,[31] or frozen orbitals.[32,33] Each of these approaches has its own advantages and disadvantages. The "best" capping method is always to choose a larger QM-cell than necessary, but this leads to increased computational costs. An alternative is the appropriate modeling of the interface region to reduce the strength and reach of the perturbations. One way to accomplish this aim is the design of optimized capping-potentials on the basis of Goedecker-type analytic pseudopotentials[34,35] (GTH-PSP), which are tuned to mimic the properties of a regular carbon-carbon

bond. In this way the chemical properties in the hybrid QM/MM calculation can be made to optimally match those in a full-QM reference calculation.

In contrast to the conventional pseudopotentials, or the effective capping-potentials by DiLabio *et al.*,[29,30] where atomic orbitals and energies of the (link) atom itself were optimized, the approach presented here tunes the capping-potentials such that the electronic density and derived quantities of the quantum fragment are preserved. It turns out, however, that it is difficult to create a capping-potential that performs equally well as a link atom for all possible capping scenarios. In particular, functional groups (e.g., polar and charged groups) may require individually optimized capping potentials. In this work, we focus on a series of biochemically relevant groups (shown in Figure 2), for which we optimize specific potentials that are well suited to retain the original electronic properties of the respective reference system.

In order to obtain a measure for the perturbations caused by our capping-potential, we define a penalty functional with contributions from the electronic density difference in the QM-region, the potential surface along the saturated bond and the force difference. The contribution from the electron density reflects the electronic ground state structure in our system. The force and energy terms are used to prevent a dissociation of the system. We test the performance of our capping-potentials with a series of structural and spectroscopic calculations, in particular NMR chemical shifts and vibrational frequencies, including a more complex hydrogen-bonded system.

II. COMPUTATIONAL DETAILS

We aim for a minimization of the electronic structure perturbation. Previous works on optimized effective core potentials[36–38] aimed at reproducing results from calculations performed with accurate, but more expensive functionals with
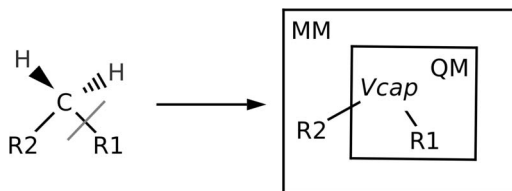
FIG. 1. The general repartitioning scheme used in QM/MM-simulations: a large system is split into two regions, a small quantum-mechanical, and a large classical box. The covalent bonds connecting the two regions must be saturated on the quantum side.

less expensive ones. In analogy to these works, we define a penalty functional measuring the deviations of several properties we are interested in

$$\mathcal{P}[\varrho] = \int_V |\varrho_{ref}(\vec{r}) - \varrho_{cap}(\vec{r})|^2 d^3r \qquad (1a)$$

$$+ \omega_F |\vec{F}_{ref} - \vec{F}_{cap}|^2 \qquad (1b)$$

$$+ \omega_E \sum_{i=1}^{3} |E_{i,ref} - E_{i,cap}|^2. \qquad (1c)$$

In this definition, Eq. (1a) is the contribution from the electronic density, Eq. (1b) measures the force acting on the capping-potential, and Eq. (1c) penalizes deviations from the potential energy surface along the covalent bond of the capping-potential. To calculate this penalty, we first compute the density and force parameters for the full reference molecule (left column in Figure 2) and for the respective
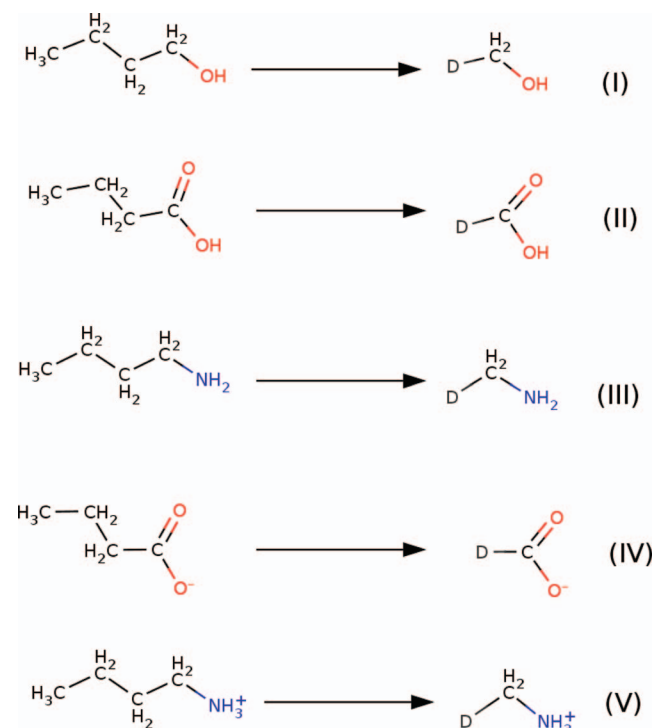

FIG. 2. The reference systems (left column) and their corresponding capped systems (right column). The capping-potential is denoted as "D".

fragment saturated by a trial capping potential (right column in Figure 2). Second, we iteratively tune the capping-potential parameters such that they eventually minimize this penalty. We use a stochastic optimization algorithm[39] for the optimization, which is based on the "artificial bee colony"-algorithm,[40–42] to avoid local minima trapping.

After completing the optimization, we compute the equilibrium geometry, potential curves, and NMR/IR-spectroscopic data to obtain properties that were not explicitly included in the penalty. This allows us to validate the properties of the capping-potentials which go beyond the electronic ground state. As a further benchmark we also calculated the performance of our capping-potentials in a hydrogen-bonded system.

It should be noted that we do not use any partial charges to represent the MM-fragment. These partial charges would clearly be important if the cleaved fragment contained polar groups; however, in our molecules, only unpolar groups are used. Nevertheless, we have specifically verified that variations of the length of the alkane chains have no significant effects on the geometry and the capping process.

All calculations were performed with the CPMD (Ref. 43) package, using a plane wave cutoff of 70 Ry, GTH-potentials for all atoms, isolated systems and the BLYP (Refs. 44 and 45) exchange-correlation functional.

III. RESULTS

A. Final potential parameters

We have optimized capping-potentials for C−C-bonds for five different molecules (see Figure 2). The potentials have the analytic form of GTH-pseudopotentials:[34]

$$V_{cap} = V_{loc} + \sum_{\ell,m} |\mathbf{R}_\ell\rangle \, |\ell m\rangle \, h_\ell \, \langle \ell m| \, \langle \mathbf{R}_\ell| ,$$

where the local potential corresponds to a smeared Gaussian charge distribution and the nonlocal part consists of a set of Gaussian projectors and spherical harmonics for several angular momentum channels. The resulting pseudopotential parameters are shown in Table I. For comparison, we also add the parameters from a previous work on C−C-capping as well as the regular carbon and hydrogen potentials. It turns out that the penalty term for the potential energy (Eq. (1c) in

TABLE I. The pseudopotentials that are optimized for different capping situations. For comparison, Komin's PSP (Ref. 46) and the regular atomic pseudopotentials for carbon and hydrogen are listed. The meaning of the different parameters is discussed in the original publication (Ref. 34).

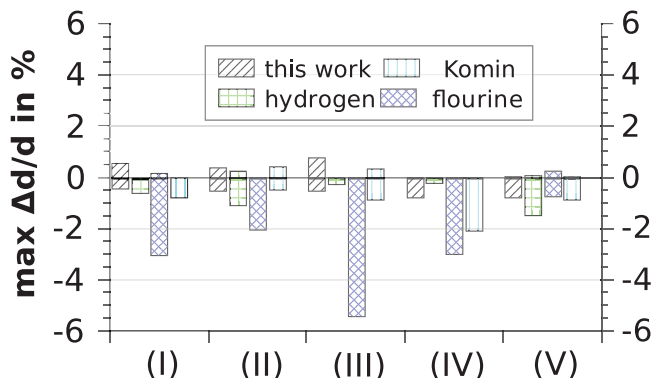| PSP	r_{loc}	C_1	C_2	r_s	$h_{s,\,11}$	r_p	$h_{p,\,11}$
(I)	0.658	8.183	–2.247	0.413	–3.252	1.420	0.152
(II)	0.692	10.307	–2.445	0.527	–3.456	1.534	0.174
(III)	0.652	7.921	–2.456	0.338	–2.942	1.297	0.219
(IV)	0.670	8.511	–2.900	0.318	–2.757	1.380	0.282
(V)	0.703	9.246	–2.195	0.504	–3.599	1.611	0.123
Komin	0.722	9.907	–2.547	0.512	–3.508	1.466	0.232
C	0.338	–9.128	1.425	0.303	9.651		
H	0.200	–4.106	0.693				

FIG. 3. Maximum relative errors of the bond lengths caused by the use of our capping-potentials and the more common fluorine- and hydrogen-capping as well as Komin's PSP in molecules I-V (see Figure 2). Both stretched and shortened covalent bonds are plotted separately. The bond with the capping-potential was not taken into account.

TABLE II. Wavenumber differences for intramolecular vibrations between carbon and the capping potential: $\Delta \tilde{v}_{cap} = \tilde{v}_{cap} - \tilde{v}_{ref}$.

System	$\Delta \tilde{v}_{cap}$ in cm^{-1}	$\Delta \tilde{v}_{Komin}$ in cm^{-1}	$\Delta \tilde{v}_{H-cap}$ in cm^{-1}
(I)	−70	−35	86
(II)	−50	−5	109
(III)	−215	−215	100
(IV)	19	N/A	92
(V)	−41	−8	100

Equation (1)) is only necessary for the butanoate ion (system (IV) in Figure 2) to avoid its dissociation, hence we could set the weighting factor ω_E to zero in all other cases. The numerical values of the capping-potentials appear to be similar across the table. However, it turns out that even small variations of the coefficients yield considerable differences in the resulting electronic densities and related properties. Hence, the different cappings are highly specific for the respective functional group for which they have been optimized.

To benchmark the quality of these capping-potentials, we have examined several properties of the capped molecules. We focus both on structural parameters and spectroscopic properties.

B. General structural properties of the capped molecules

We have performed geometry optimizations of the capped molecules and analyzed the bond lengths and bond angles of the remaining atoms. The results are shown in Figure 3. Our pseudopotentials reproduce the geometry of

the original system very well, the deviations are consistently below 1%. Hydrogen-capping often leads to comparable results, but for, e.g., butanoic-acid and butan-aminium it causes larger errors. The carbon-dummy bond was excluded because of the large discrepancies between a C−C-bond and a C−H, or C−F-bond. Nevertheless, it should be mentioned that our capping-potentials also cause no significant error in this bond, except for the butanoate-ion. An analysis of the bond angles (data not shown) did not show any deviations above 5°.

We have further examined the potential curve of the C−D-bond (shown in Figure 4) to ensure that the capped molecule will not dissociate. The qualitative behavior of the reference is reproduced very well up to a distance of 1.8 Å. Our capping-potentials and Komin's PSP cause, in most cases, a redshift in the vibrational spectrum, in contrast to this hydrogen-capping causes a blueshift. The wavenumber differences, which are listed in Table II, were calculated by fitting the harmonic part of the energy curves, where we assumed the reduced mass of a carbon-carbon bond. Our capping-potential optimized for the butanoate-ion (IV) causes a shortened equilibrium bond length and a flatter potential surface. In comparison, Komin's PSP yields a potential curve without a minimum, leading to an easy dissociation of the molecule. Our capping-potentials show slightly higher deviations from the reference than Komin's PSP, but, except for butylamine, are still closer to the reference than hydrogen-capping. This is because in the previous work by Komin and Sebastiani,[46] a higher emphasis was put on geometrical properties of the saturated bond, while the focus in the present work is mainly on the electronic structure within in the functional group.
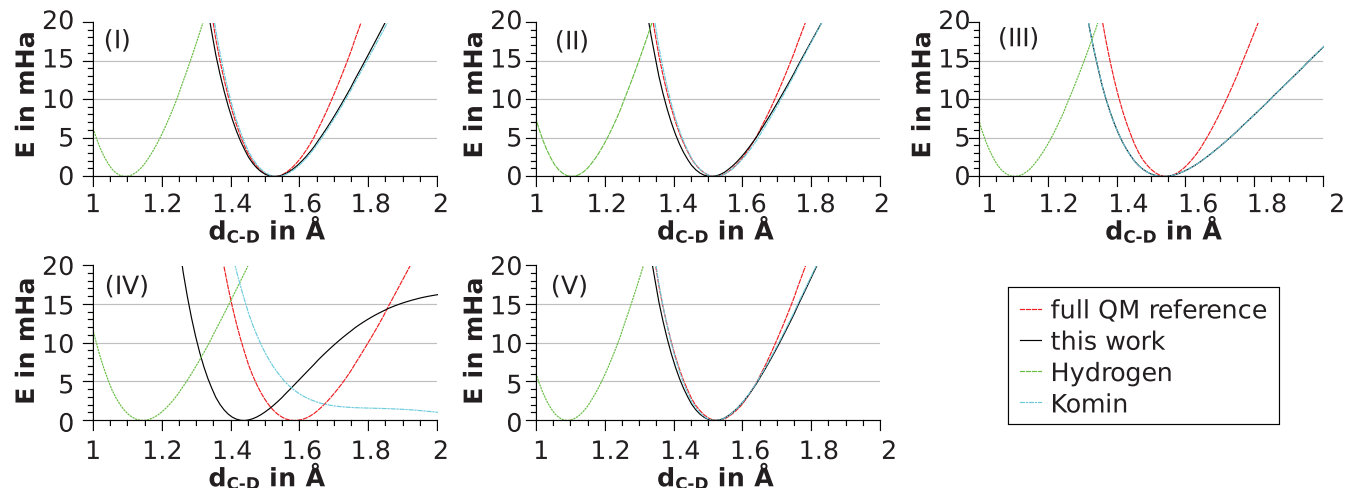

FIG. 4. Potential curves for the bond between the carbon atom and the capping-potential (after full relaxation of the remaining degrees of freedom). The zero-point of the energy scale is set to the energy of the equilibrium structure.
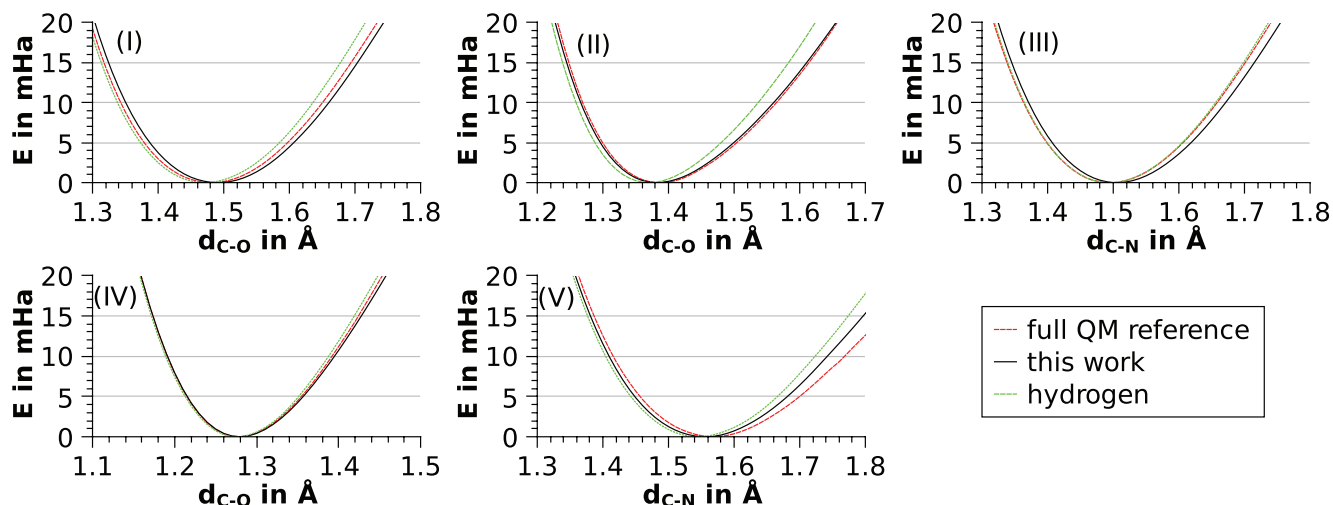
FIG. 5. Potential curves for the bond between the carbon atom and the nitrogen/oxygen-atom in the functional group, using a geometry-optimized structure. The zero-point of the energy scale is set to the energy of the relaxed structure. For the carboxylic acid the single-bonded oxygen atom was examined.

In addition to the C−D-bond, we also examined the potential curve of the carbon and its neighboring nitrogen or oxygen. Figure 5 shows the energy curves for the bond between the remaining carbon atom in the QM-zone and, depending on the system, either an oxygen or nitrogen atom. Our capping-potentials reproduce the qualitative behavior of all of these bonds very well.

C. Spectroscopic properties

Equilibrium distances and potential curves of covalent bonds are crucial properties for obtaining structural and dynamical properties of complex systems within MD simulations. However, at least equally important are spectroscopic observables which provide a link to experimental results.[47, 48] Among the most commonly used techniques in experiment and theory are IR, Raman, UV-vis, NMR, and EPR spectroscopy. All of these methods involve the (linear) response of the electronic structure to external fields.[49–51] Hence, they depend not only on the electronic ground state but also on excited states of the system. Therefore, we have complemented the analysis of our capping-potentials with the investigation of their performance in view of vibrational spectra and chemical shifts from NMR.

To investigate the vibrational properties of the molecules, we fitted the harmonic part of the potential curves shown in

Figure 5 with $E(d) = \mu(2\pi\tilde{v}c)^2(d - d_0)^2$. μ denotes the reduced mass of the carbon atom and the oxygen or respectively the nitrogen atom. The resulting wavenumbers are listed in Table III.

From those results it can be seen that our capping-potentials reproduce the original vibrational behavior very well. Except for the butanoate-ion, they are closer to the reference value than hydrogen-capping. In difference to hydrogen-capping, which causes a blueshift in all examined systems, our capping potential approach does not show a systematic shift in one direction.

Finally, we compute the chemical shifts for all atoms in the QM-zone and compare them to our reference calculations. In Figure 6, the differences of the chemical shifts between the capped system and a full quantum reference calculation are shown for various capping-potentials. For the calculation of the chemical shifts in the capped systems we used the re-optimized geometry as well as the geometry that was used for the capping-potential optimization. The errors of the NMR chemical shifts for hydrogen are on the same scale as those of Komin's pseudopotential and hydrogen capping, when using a re-optimized geometry. The deviations that arise from our capping-potentials for the carbon and oxygen atoms on the other hand are often significantly smaller than those from hydrogen-capping or Komin's potential. For nitrogen atoms, we achieve results that are close to Komin's PSP, but better than hydrogen-capping. In Table IV, we list the root mean square errors for the different systems and capping methods.

TABLE III. Wavenumber differences ($\Delta\tilde{v}_{cap} = \tilde{v}_{cap} - \tilde{v}_{ref}$) for intramolecular vibrations between carbon and either oxygen or nitrogen. For butanioc-acid, the single-bonded oxygen was evaluated.

System	$\tilde{v}_{ref}$ in cm^{-1}	$\tilde{v}_{cap}$ in cm^{-1}	$\tilde{v}_{H-cap}$ in cm^{-1}	$\Delta\tilde{v}_{cap}$ in cm^{-1}	$\Delta\tilde{v}_{H-cap}$ in cm^{-1}
(I)	655	660	668	5	13
(II)	718	714	723	−4	5
(III)	728	726	735	−2	7
(IV)	1077	1068	1077	−9	0
(V)	653	665	679	12	16

TABLE IV. RMSE of the chemical shifts shown in Figure 6.

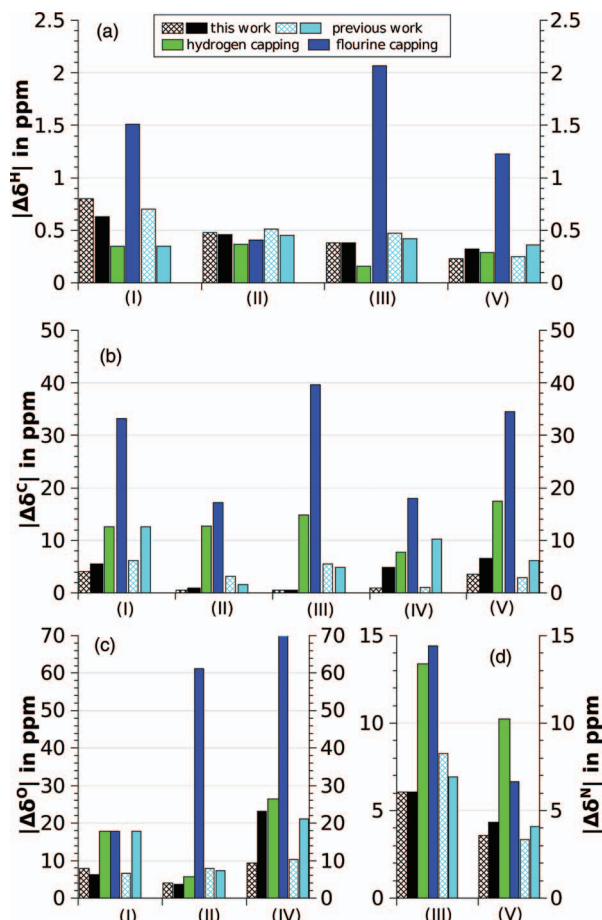| System	RMSE$_{cap}$ in ppm	RMSE$_{H-cap}$ in ppm	$RMSE_{Komin}$ in ppm
(I)	3.78	9.79	3.75
(II)	3.68	7.66	5.43
(III)	2.51	8.16	3.47
(IV)	3.94	22.30	20.10
(V)	2.97	7.66	2.81

FIG. 6. Average absolute errors in the chemical shifts (a) hydrogen, (b) carbon, (c) oxygen, and (d) nitrogen) caused by the capping. Shown are the errors for our optimized potentials, fluorine, and hydrogen cappings, as well as a potential from previous work done by Komin and Sebastiani.[46] The striped bars represent the geometry that was used for finding the capping-potential, the solid bars show the results for the re-optimized geometry.

IV. APPLICATION

The set of optimized capping-potentials described above perform in many ways better than hydrogen-capping within the simple testing systems they were optimized for. To check whether they perform equally well in more complex cases, we apply them to a hydrogen-bonded system and calculate the proton affinities of the reference systems.[52,53]

TABLE V. Properties of the hydrogen bonds computed by using our capping-potential or hydrogen capping, compared with the full quantum reference (calculated as $X_{cap} - X_{ref}$). The atomic labels are shown in Figure 7. A negative ΔE_{H-bond} represents a more attractive hydrogen bond.

	This work	H - Capping
$\Delta d(C_1 - C_2)$ in pm	0	−6
$\Delta d(O_1 - O_4)$ in pm	0	−2
$\Delta d(O_2 - O_3)$ in pm	1	−3
$\Delta d(O_3 - H_1)$ in pm	1	−4
$\Delta d(O_1 - H_2)$ in pm	1	−2
ΔE_{H-bond} in mHa	0.95	−1.56
ΔE_{H-bond} in %	3.3	−5.5

A. Hydrogen-bonded systems

To check the performance of our capping-potentials in hydrogen-bonded systems, we apply them to a butanoic-acid dimer, as shown in Figure 7. Here, we focus on the hydrogen bonds, which we analyze by means of characteristic atomic distances, the energy gain from the hydrogen bond formation, and the shape of the potential curve for the $C_1 - C_2$ distance. Furthermore, we compute the chemical shifts in order to determine short range perturbations in the domain of the hydrogen-bond as well as long-range perturbations in the remaining alkyl chain.

In Table V, we show the atomic distances characteristic for the hydrogen bond and the energy of the hydrogen bond. In contrast to hydrogen capping, which causes slight geometrical perturbations, our capping-potential causes almost no perturbation to the structure of the hydrogen bonds. In addition, our capping-potential also features a lower error in the dissociation energy. The energy as a function of the $C_1 - C_2$ distance is shown in Figure 8. Our capping-potential is closer to the reference at long distances, while hydrogen-capping performs better at short distances (relative to the equilibrium distance). Hence, neither of the capping methods reproduces the reference curve perfectly. We have further computed the harmonic frequencies of a fictitious intermolecular mode, assuming rigid butanoic-acid molecules (shown in Table VI).

The significant difference between the two capping methods indicates, that our potential reproduces the potential curve better around the equilibrium distance.
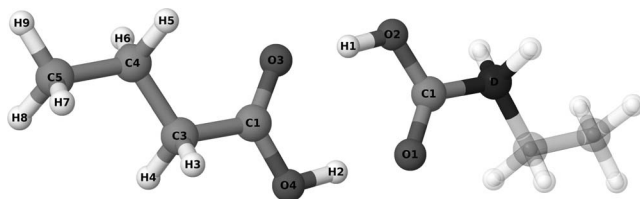

FIG. 7. Two butanoic-acid molecules with hydrogen bonds, which we used to benchmark our capping-potentials. The translucent atoms are only included in the reference calculation. The carbon atom drawn in dark gray represents the cleavage site.
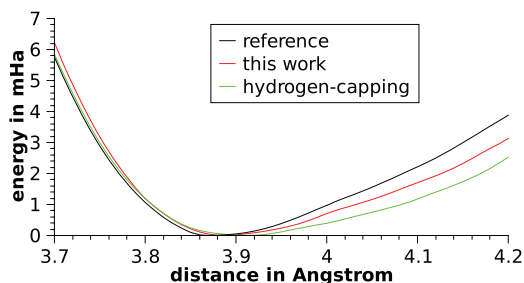

FIG. 8. Potential curve for the C_1-C_2 distance of the application setup shown in Figure 7. Shown are the reference calculation, our capping-potential and hydrogen-capping. For the calculation equilibrated geometries were used and the energy zero point is set to the minimum energy.

TABLE VI. Wavenumbers for the intermolecular mode of the butanoic-acid dimer, assuming rigid molecules.

$\tilde{v}_{ref}$	$\tilde{v}_{cap}$	$\tilde{v}_{H-cap}$
175.8 cm^{-1}	180.2 cm^{-1}	150.7 cm^{-1}

In addition, we calculated the chemical shifts, which are listed in Table VII. We show the shifts explicitly for the atoms close to the hydrogen bonds, for the remaining alkyl-chain (beginning at C_3 in Figure 7), we list the average of the absolute errors as a measure for the spread of the perturbations.

Both capping methods cause no significant long-range perturbations and almost no errors in the NMR chemical shifts of the hydrogen atoms. However, our approach is able to reduce the errors of the carbon chemical shifts. On the short-range scale, the difference between the capping methods becomes more obvious. Our approach significantly reduces the perturbations caused on the capped side, e.g., the error of the hydrogen atom is reduced to less than one third of the H-capping error. The other functional group shows a similar behavior, except for O_4, where we have an increment of the error by $\approx$ 1ppm, all errors are reduced; the perturbation at H_2 is reduced to less than one fourth compared to the H-capping situation. In total, we are able to reduce the RMSE of the chemical shifts from 4.11ppm (H-Capping) to 2.11 ppm.

B. Proton affinities

We have checked whether our capping-potentials cause a significant change in the proton affinity $E_{pa} = E(A^-) - E(HA)$ of the functional group they are designed for. Specifically, we applied the potentials we found for the butanoic acid ((II) in Figure 2) and the butylamine (III) to their charged counterparts (IV) and (V), and vice versa. The resulting energy differences are listed in Table VIII.

When using the capping-potentials optimized for the protonated acid and amine groups, $V_{(II)}$ and $V_{(V)}$, we obtain smaller errors in proton affinities compared to hydrogen-capping. This does not hold for the capping-potentials obtained on the basis of the corresponding deprotonated groups. Here, one of them ($V_{(IV)}$) exhibits an error, that is twice as large as the hydrogen capping. In general H-capping tends to weaken the proton affinity of the system, while our cappings mostly increase the proton affinity. For all capping methods

TABLE VII. The deviations of the chemical shifts in the capped system caused by our capping-potential and hydrogen-capping. For the carbon and hydrogen atoms that are not listed explicitly, we have taken the average of the absolute errors.

	$\delta_{cap} - \delta_{ref}$ in ppm			$\delta_{cap} - \delta_{ref}$ in ppm	
Atom label	This work	H-capping	Atom label	This work	H-Capping
C_1	1.42	−11.66	O_1	1.6	5.6
C_2	0.15	0.43	O_2	8.38	11
H_1	−0.29	1.02	O_3	2.03	−3.74
H_2	0.07	0.33	O_4	0.94	0.05
$\langle|C|\rangle$	0.04	0.33	$\langle|H|\rangle$	0.01	0.01

TABLE VIII. The deviations in the proton affinities E_{pa} (calculated as $E_{pa,\,cap} - E_{pa,\,ref}$) for the butanoate-ion and butylamine, computed using our capping potentials as well as hydrogen-capping. A positive ΔE_{pa} indicates a stronger proton affinity than the reference.

	ΔE_{pa} in mHa for capping potential				
	$V_{(II)}$	$V_{(III)}$	$V_{(IV)}$	$V_{(V)}$	H-Capping
acids (II)/(IV)	−4.25	N/A	14.11	N/A	−6.04
amines (III)/(V)	N/A	6.23	N/A	3.65	−9.65

the relative errors are below 3%, so that the overall impact is moderate.

V. DISCUSSION AND CONCLUSIONS

We have computed a series of capping-potentials for hybrid quantum/classical (QM/MM) calculations. Each capping is specifically optimized for accurately saturating the quantum fragments of a given polar group. We have applied this to a representative set of groups which are often encountered in biomolecules and functional materials.

We found these potentials to reduce the perturbations of the electronic structure compared to the more common hydrogen-capping. Both capping-methods cause only small changes of the molecular geometry, but our approach leads to better spectroscopic results. Except for butanoic-acid, we obtain vibrational frequencies closer to the reference with our approach. In all examined systems, we find the same order of magnitude for the error of the hydrogen chemical shifts, but in many cases a reduction of several ppm for carbon, oxygen and nitrogen atoms. This is remarkable, because our optimization procedure only takes into account ground state properties, while chemical shifts also depend on excited states. Transferring our capping-potentials to a hydrogen-bonded system, we find again only little influence on the geometry. Also in this setup, our approach produces smaller errors in the chemical shifts than hydrogen-capping. Furthermore, our capping-potentials reduces the dissociation energy error by one third. We also evaluated the proton affinities of butanoate-ion and butylamine and found most of our capping-potentials to reproduce this property better than H-capping does. These results show that QM/MM interface regions close to functional groups should be terminated with specifically optimized capping-potentials to improve spectroscopic results. These capping-potentials also keep deviations minimal when the fragments are involved in hydrogen bonds. To further improve the quality of our capping-potentials, we aim at also including excited states in the penalty functional, mainly in view of linear response properties. The quality of the proton affinities could be further improved by including this property directly into the penalty functional.

ACKNOWLEDGMENTS

[1]T. Christen, P. Hunenberger, D. Bakowies, R. Baron, R. Burgi, D. Geerke, T. Heinz, M. Kastenholz, V. Krautler, C. Oostenbrink, C. Peter, D. Trzesniak, and W. F. van Gunsteren, J. Comput. Chem. **26**, 1719 (2005).

[2]D. P. Geerke, S. Thiel, W. Thiel, and W. F. van Gunsteren, Phys. Chem. Chem. Phys. **10**, 297 (2008).

[3]Y. Duan and P. A. Kollman, Science **282**, 740 (1998).

[4]P. A. Kollman, Chem. Rev. **93**, 2395 (1993).

[5]W. L. Jorgensen, J. Chandrasekhar, J. D. Madura, R. W. Impey, and M. L. Klein, J. Chem. Phys. **79**, 926 (1983).

[6]D. Chandler, J. Chem. Phys. **68**, 2959 (1978).

[7]A. Alavi, J. Kohanoff, M. Parrinello, and D. Frenkel, Phys. Rev. Lett. **73**, 2599 (1994).

[8]R. Car and M. Parrinello, Phys. Rev. Lett. **55**, 2471 (1985).

[9]K. Laasonen, M. Sprik, M. Parrinello, and R. Car, J. Chem. Phys. **99**, 9080 (1993).

[10]G. Lippert, J. Hutter, and M. Parrinello, Theor. Chem. Acc. **103**, 124 (1999).

[11]D. Sebastiani, Nachr. Chem., Tech. Lab. **57**, 305 (2009).

[12]R. O. Jones and O. Gunnarsson, Rev. Mod. Phys. **61**, 689 (1989).

[13]G. Brancato, N. Rega, and V. Barone, J. Chem. Phys. **128**, 144501 (2008).

[14]Q. Cui, J. Chem. Phys. **117**, 4720 (2002).

[15]Q. Cui and M. Karplus, J. Chem. Phys. **112**, 1133 (2000).

[16]R. Z. Deng, G. J. Martyna, and M. L. Klein, Phys. Rev. Lett. **71**, 267 (1993).

[17]M. Eichinger, P. Tavan, J. Hutter, and M. Parrinello, J. Chem. Phys. **21**, 10452 (1999).

[18]P. Lyne, M. Hodosceck, and M. Karplus, J. Phys. Chem. A **103**, 3462 (1999).

[19]M. J. Field, P. A. Bash, and M. Karplus, J. Comput. Chem. **11**, 700 (1990).

[20]P. Sherwood, A. H. de Vries, M. F. Guest, G. Schreckenbach, C. R. A. Catlow, S. A. French, A. A. Sokol, S. T. Bromley, W. Thiel, A. J. Turner, S. Billeter, F. Terstegen, S. Thiel, J. Kendrick, S. C. Rogers, J. Casci, M. Watson, F. King, E. Karlsen, M. Sjovoll, A. Fahmi, A. Schafer, and C. Lennartz, J. Mol. Struct.: THEOCHEM **632**, 1 (2003).

[21]H. M. Senn and W. Thiel, Top. Curr. Chem. **268**, 173 (2007).

[22]T. Benighaus and W. Thiel, J. Chem. Theory Comput. **4**, 1600 (2008).

[23]U. Rohrig, L. Guidoni, and U. Rothlisberger, ChemPhysChem **6**, 1836 (2005).

[24]J. Pu, J. Gao, and D. G. Truhlar, J. Phys. Chem. A **108**, 632 (2004).

[25]J. Jung, C. H. Choi, Y. Sugita, and S. Ten-no, J. Chem. Phys. **127**, 204102 (2007).

[26]A. Laio, J. VandeVondele, and U. Roethlisberger, J. Chem. Phys. **116**, 6941 (2002).

[27]U. C. Singh and P. A. Kollman, J. Comput. Chem. **7**, 718 (1986).

[28]Y. Zhang, T.-S. Lee, and W. Yang, J. Phys. Chem. **110**, 46 (1999).

[29]G. A. DiLabio, M. M. Hurley, and P. A. Christiansen, J. Chem. Phys. **116**, 9578 (2002).

[30]G. A. DiLabio, R. A. Wolkow, and E. R. Johnson, J. Chem. Phys. **122**, 044708 (2005).

[31]J. Gao, P. Amara, C. Alhambra, and M. J. Field, J. Phys. Chem. A **102**, 4714 (1998).

[32]X. Assfeld and J.-L. Rivail, Chem. Phys. Lett. **263**, 100 (1996).

[33]C. R. Jacob and L. Visscher, J. Chem. Phys. **125**, 194104 (2006).

[34]S. Goedecker, M. Teter, and J. Hutter, Phys. Rev. B **54**, 1703 (1996).

[35]C. Hartwigsen, S. Goedecker, and J. Hutter, Phys. Rev. B **58**, 3641 (1998).

[36]O. A. von Lilienfeld, I. Tavernelli, U. Rothlisberger, and D. Sebastiani, J. Chem. Phys. **122**, 014113 (2005).

[37]O. A. von Lilienfeld, I. Tavernelli, U. Rothlisberger, and D. Sebastiani, Phys. Rev. B **71**, 195119 (2005).

[38]O. A. von Lilienfeld, I. Tavernelli, U. Rothlisberger, and D. Sebastiani, Phys. Rev. Lett. **93**, 153004 (2004).

[39]C. Schiffmann and D. Sebastiani, J. Chem. Theory Comput. **7**, 1307 (2011).

[40]D. Karaboga and B. Basturk, J. Global Optim. **39**, 459 (2007).

[41]D. Karaboga and B. Basturk, Appl. Soft Comput. **8**, 687 (2008).

[42]D. Karaboga and B. Akay, Artif. Intell. Rev. **31**, 61 (2009).

[43]J. Hutter, D. Marx, P. Focher, M. Tuckerman, W. Andreoni, A. Curioni, E. Fois, U. Rothlisberger, P. Giannozzi, T. Deutsch, A. Alavi, D. Sebastiani, A. Laio, J. Vandevondele, A. Seitsonen, S. Billeter, and M. Parinello, CPMD, version 3.13.2 (IBM Corp. and MPI-FKF Stuttgart, 2010).

[44]A. D. Becke, Phys. Rev. A **38**, 3098 (1988).

[45]C. Lee, W. Yang, and R. G. Parr, Phys. Rev. B **37**, 785 (1988).

[46]S. Komin and D. Sebastiani, J. Chem. Theory Comput. **5**, 1490 (2009).

[47]H. J. Bakker and J. L. Skinner, Chem. Rev. **110**, 1498 (2010).

[48]J. Schmidt, A. Hoffmann, H. W. Spiess, and D. Sebastiani, J. Phys. Chem. B **110**, 23204 (2006).

[49]S. Baroni, S. de Gironcoli, A. del Corso, and P. Giannozzi, Rev. Mod. Phys. **73**, 515 (2001).

[50]A. Putrino, D. Sebastiani, and M. Parrinello, J. Chem. Phys. **113**, 7102 (2000).

[51]D. Sebastiani and M. Parrinello, J. Phys. Chem. A **105**, 1951 (2001).

[52]P. H. König, M. Hoffmann, T. Frauenheim, and Q. Cui, J. Phys. Chem. B **109**, 9082 (2005).

[53]D. Das, K. P. Eurenius, E. M. Billings, P. Sherwood, D. C. Chatfield, M. Hodoscek, and B. R. Brooks, J. Chem. Phys. **117**, 10534 (2002).